Modeling and Control of Excavator Dynamics during Digging Operation

By A. J. Koivo,[1] M. Thoma,[2] E. Kocaoglan,[3] and J. Andrade-Cetto[4]

Abstract: Automation of excavation operations can be realized by an automatically controlled excavator system that is able to perform autonomously a planned digging work and to quickly comply to interacting forces experienced during excavation. The development of such an automated control system is usually based on a dynamic model of the system that describes the motion with time. A dynamic model for an excavator that is needed for the controller design can be derived by applying Newton-Euler equations to each link in succession. The model obtained describes the motion of the excavator. It corrects several shortcomings that appear in previously published excavator model. On the basis of the model derived, a proportional-differential controller is designed that makes the bucket to track a specified trajectory. It can be used to automate the machine operations, for example, for terrestrial and planetary excavations as well as for mining applications.

INTRODUCTION

A control system can be designed to automate excavator operations. During the digging task, it must control not only the bucket trajectory but also the forces exerted by the bucket (end-effector) on the soil. In order to design a controller for an excavator system, a dynamic model describing its behavior is necessary. The equations of motion of the excavator in the chosen coordinate systems can be derived by applying commonly accepted approaches of robotics, for example, by forming Euler-Lagrange's equations from Lagrange's energy function, or by writing Newton-Euler's equations for each link of the system in succession.

The application of Euler-Lagrange's equation gives the designer physical insight needed to understand the behavior of the overall system, but the resulting equations are often computationally complex. On the other hand, the application of Newton-Euler's equations gives a computationally attractive model in which the dynamics of each link are described by a recursive relation relative to the link index. The driving joint torques of the excavator mechanisms are generated by the forces of the hydraulic rams (the actuators). The dynamic model obtained describes the translational and rotational motions of the serially connected links, i.e., the dynamics of the upper structure, the boom, the arm, and the bucket in the excavator system.

The kinematic modeling of excavators has been reported in the literature; for example, the kinematic equations of the positioning (Khoshzaban et al. 1992; Koivo 1994) and the static force/torque relations (Bullock et al. 1990; Bernold 1991; Hemami and Daneshmend 1992). On the other hand, the dynamic modeling of excavators has attracted little attention. Preliminary work on modeling the dynamics of excavators has been presented (Vähä et al. 1991); however, the modeling is incomplete. A later attempt to describe an excavator model is presented in Vähä and Skibniewski (1993); however, the model developed is untractable. In fact, its interpretation raises queries in general; for example, many variables are undefined.

The purpose here is to present a complete dynamic model for excavators. The inputs consist of the forces generated by the hydraulic actuators, i.e., the rams, and the output is the pose (position and orientation) of the bucket. The forces acting between the bucket and the soil during the digging operations are also included in the dynamic model.

The presentation of the paper is organized as follows: First the brief description of the kinematics and coordinate assignments are given. Then, the equations of motion for the links in recursive forms are written using Newton-Euler equations. The resulting dynamic model of the excavator are presented and discussed. Finally, simulations of the implementation of a PD controller are presented in order to illustrate the use of the dynamic model.

KINEMATICS

To describe the positions of the points on an excavator, the designer defines Cartesian (i.e., rectangular and right-handed) coordinate systems attached to the links, and a fixed Cartesian (world) coordinate system with the origin on the body of the excavator (see Figs. 1a and 1b). The coordinate systems are assigned systematically by applying Denavit and Hartenberg procedure described for excavators in Koivo (1994). A possible assignment of the coordinate frames for the mechanism is shown in Fig. 1(b). It may be noticed that the rotational axis for the first link (i.e., the supporting base) is vertical, whereas the rotational axes for the other links are horizontal. The nomenclature used in the sequel is presented in Appendix VI.

For determining the transformation matrices that relate the representations in two adjacent coordinate frames, the structural kinematic parameters d_i, a_i, α_i, and θ_i, $i = 1, \ldots, 4$ for the links are first defined. They are presented in Table 1 for the system in Fig. 1(b).

The transformation matrix relating two adjacent [ith and $(i-1)$th] coordinate frames is as follows:

$$\mathbf{A}_{i-1}^{i} = \begin{bmatrix} \cos\theta_i & -\cos\alpha_i \sin\theta & \sin\alpha_i \sin\theta_i & a_i \cos\theta_i \\ \sin\theta_i & \cos\alpha_i \cos\theta_i & -\sin\alpha_i \cos\theta_i & a_i \sin\theta_i \\ 0 & \sin\theta_i & \cos\alpha_i & d_i \\ 0 & 0 & 0 & 1 \end{bmatrix} \tag{1}$$

It follows then that vector ${}^{i}\mathbf{p}$ in the ith coordinate system and vector ${}^{i+1}\mathbf{p}$ in the $(i+1)$th coordinate frame, $i = 0, 1, 2, 3$, are related by

$${}^{i}\mathbf{p} = \mathbf{A}_{i}^{i+1}({}^{i+1}\mathbf{p}) \tag{2}$$

[1]Prof., School of Electr. Engrg., Purdue Univ., West Lafayette, IN 47907; formerly, Visiting Alexander von Humboldt Foundation Senior Researcher, Inst. für Regelungstechnik, Univ. of Hannover, Hannover, Germany.

[2]Prof., Inst. für Regelungstechnik, Univ. of Hannover, Hannover, Germany.

[3]Prof., Middle East Tech. Univ., Ankara, Turkey.

[4]Centro de Enseñanza Técnica y Superior (CETYS) Universidad, Mexicali, Baja California Norte, Mexico.

Note. Discussion open until June 1, 1996. To extend the closing date one month, a written request must be filed with the ASCE Manager of Journals. The manuscript for this paper was submitted for review and possible publication on May 17, 1994. This paper is part of the ***Journal of Aerospace Engineering***, Vol. 9, No. 1, January, 1996. ©ASCE, ISSN 0893-1321/96/0001-0010–0018/$4.00 + $.50 per page. Paper No. 8451.

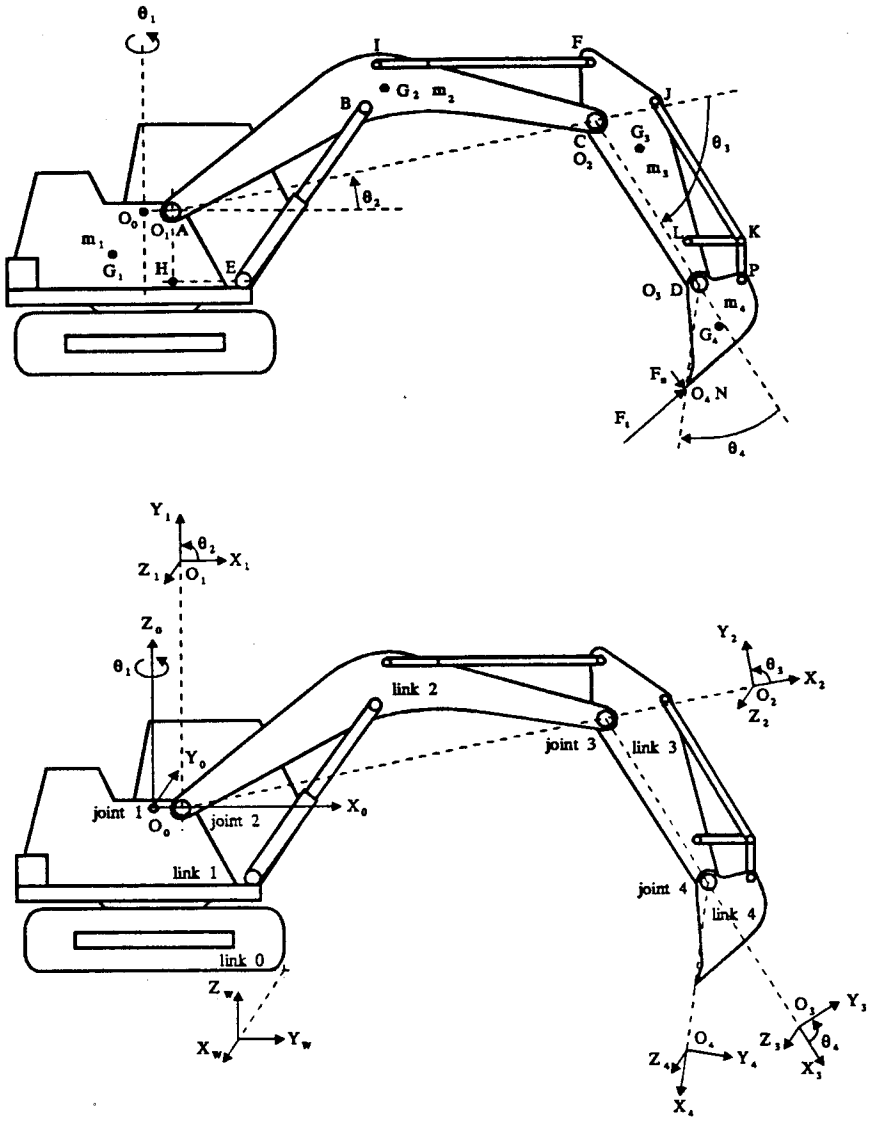

FIG. 1. Excavator: (a) Side View; (b) Coordinate Frames

TABLE 1. Structural Kinematic Parameters

Link i (1)	d_i (2)	a_i (3)	α_i (4)	θ_i (5)
1	0	$a_1 = l_1$	90	θ_1
2	0	$a_2 = l_2$	0	θ_2
3	0	$a_3 = l_3$	0	θ_3
4	0	$a_4 = l_4$	0	θ_4

which can be used to relate the vectors for the bucket pose (position and orientation) in the base and fourth coordinate systems (Fig. 2). Thus, vector ${}^4\mathbf{p}$ in the fourth coordinate frame and vector ${}^0\mathbf{p}$ in the base coordinate system are related as

$$ {}^0\mathbf{p} = \mathbf{A}_0^4({}^4\mathbf{p}) \tag{3} $$

where $\mathbf{A}_0^4 = \mathbf{A}_0^1\mathbf{A}_1^2\mathbf{A}_2^3\mathbf{A}_3^4$; and $(\mathbf{A}_0^4)^{-1} = \mathbf{A}_4^0$. If ${}^4\mathbf{p}$ specifies the center point of the bucket edge in the fourth coordinate system, i.e., ${}^4\mathbf{p} = [0\ 0\ 0\ 1]^T$, then the same position in the base coordinate system is ${}^0\mathbf{p} = \mathbf{A}_0^4({}^4\mathbf{p})$.

The bucket pose is related to the joint angles. The joint angles can then be expressed in terms of the lengths (line segments) of the hydraulic actuators (rams). These relationships together establish the usual kinematic pose equations

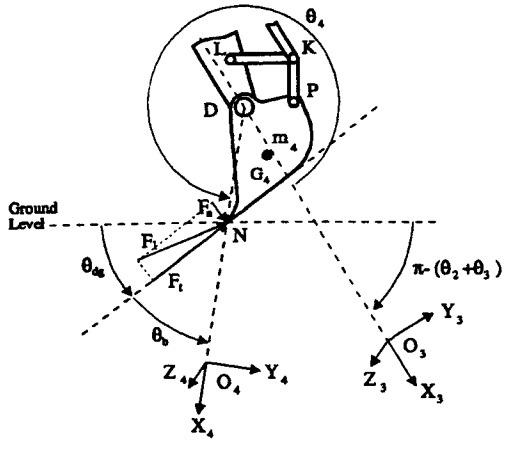

FIG. 2. Excavator Bucket

of the mechanism. They are presented in detail in Koivo (1994), and are not repeated here.

A dynamic model for an excavator is next presented by applying Newton-Euler equations of motion to each link (i.e., a free body) of the machine.

EQUATIONS OF MOTION

The dynamic model for an excavator will be described next. For convenience, the dynamic model for the excavator is presented in the digging mode, that is, the rotation angle θ_1 of the first link is held constant. It follows that the movements of the excavator mechanism during the digging occur in the vertical plane. The equations of the motion can then be derived in a standard manner, and can be found in the common textbooks on introductory robotics [e.g., Koivo (1989)]. The model equations are written for each link of the excavator by considering the links as free bodies shown in Fig. 3.

First, the equations are determined for the velocities and accelerations of all links in the local coordinate frames. Then, the corresponding variables for the centroids of the links are obtained. The foregoing equations for the velocities and accelerations of the excavator links are presented in detail in Appendix I and summarized here.

The rotational and translational velocities and accelerations for each link are described in recursive forms as follows:

$$ {}^{i+1}\vec{\omega}_{0(i+1)} = {}^{i+1}\vec{\omega}_{0i} + \dot{\theta}_{i+1}({}^{i+1}\vec{k}_{zi}) \tag{4} $$

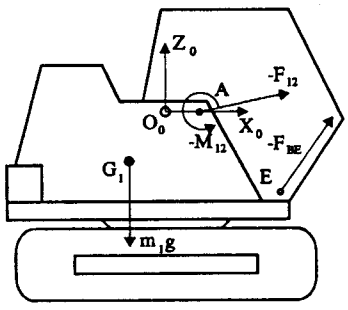

(a) Link 1

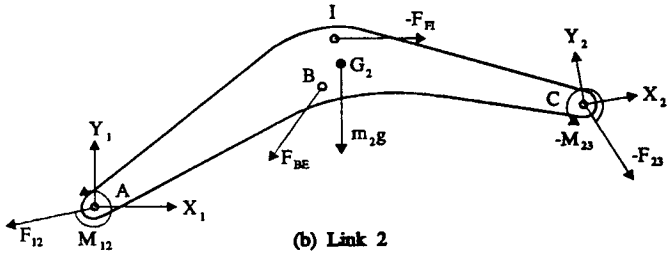

(b) Link 2

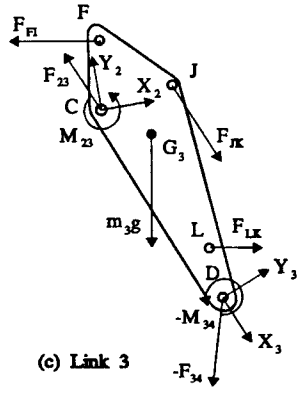

(c) Link 3

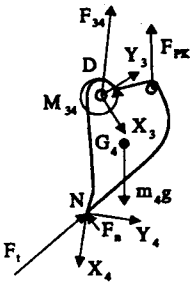

(d) Link 4

FIG. 3. Free Body Diagrams: (a) Link 1, Upper Structure; (b) Link 2, Boom; (c) Link 3, Arm; (d) Link 4, Bucket

where $i = 0, 1, 2, 3$; ω_{0i} specifies the rotational velocity of link i in the base coordinate frame; and ${}^{i+1}\omega_{0i}$ in the $(i + 1)$th coordinate frame. Moreover, ${}^{i+1}\omega_{0i} = (\mathbf{R}^i_{i+1})(\mathbf{R}^0_i)\omega_{0i}$ with $\mathbf{R}^i_{i+1} = (\mathbf{A}^i_{i+1})_R$ being the rotation submatrix of the homogeneous transformation matrix $\mathbf{A}^i_{i+1}$ that relates a vector in the ith coordinate frame to a vector in the $(i + 1)$th coordinate frame (Koivo 1994). $\dot{\theta}_{i+1}$ is the rotational velocity of link $(i + 1)$ relative to the previous link about the (positive) Z_i-axis and measured from the positive X_i-axis to the counterclockwise direction.

Similarly, the translational velocity $\mathbf{v}_{0(i+1)}$ of the origin of the $(i + 1)$th coordinate frame (i.e., the distal end-point of link $i + 1$) is specified in the $(i + 1)$th coordinate frame as

$$ {}^{i+1}\vec{v}_{0(i+1)} = {}^{i+1}\vec{v}_{0i} + {}^{i+1}\vec{\omega}_{0(i+1)} \times [{}^{i+1}\vec{p}_{0(i+1)} - {}^{i+1}\vec{p}_{0i}] \tag{5} $$

where ${}^{i+1}\vec{p}_{0i}$ = vector from the origin of the base coordinate system to the origin of the ith coordinate frame expressed in the $(i + 1)$th coordinate system; and the "$\times$" represents a cross-product operation.

The corresponding expression for the rotational acceleration is as follows:

$$ {}^{i+1}\vec{\alpha}_{0(i+1)} = {}^{i+1}\vec{\alpha}_{0i} + \ddot{\theta}_{i+1}({}^{i+1}\vec{k}_{zi}) \tag{6} $$

where ${}^{i+1}\vec{\alpha}_{0i} = {}^{i+1}\dot{\vec{\omega}}_{0i}$ is the rotational acceleration of the origin of the ith coordinate frame expressed in the $(i + 1)$th coordinate system.

The translational acceleration ${}^{i+1}\mathbf{a}_{0(i+1)} = {}^{i+1}\dot{\mathbf{v}}_{0(i+1)}$ of the origin of the $(i + 1)$th coordinate frame expressed in the $(i + 1)$th coordinate system is

$$ {}^{i+1}\vec{a}_{0(i+1)} = {}^{i+1}\vec{a}_{0i} + [{}^{i+1}\vec{\alpha}_{0(i+1)}] \times ({}^{i+1}\vec{p}^{\,*}_{i+1}) + [{}^{i+1}\vec{\omega}_{0(i+1)}] \times \{[{}^{i+1}\vec{\omega}_{0(i+1)}] \times ({}^{i+1}\vec{p}^{\,*}_{i+1})\} \tag{7} $$

where ${}^{i+1}\vec{p}^{\,*}_{i+1} = {}^{i+1}\vec{p}_{0(i+1)} - {}^{i+1}\vec{p}_{0i}$ describes the position of the origin of the ith coordinate frame in the $(i + 1)$th coordinate system.

The translational velocity ${}^i\mathbf{v}_{0Gi}$ and acceleration ${}^i\mathbf{a}_{0Gi}$ of the gravity center G_i of link i are then defined by

$$ {}^i\vec{v}_{0Gi} = {}^i\vec{v}_{0i} + {}^i\vec{\omega}_{0i} \times {}^i\vec{p}^{\,*}_{Gi} \tag{8} $$

$$ {}^i\vec{a}_{0Gi} = {}^i\vec{a}_{0i} + {}^i\vec{\alpha}_{0i} \times {}^i\vec{p}^{\,*}_{Gi} + {}^i\vec{\omega}_{0i} \times ({}^i\vec{\omega}_{0i} \times {}^i\vec{p}^{\,*}_{Gi}) \tag{9} $$

where ${}^ip^*_{Gi} = \mathbf{R}^0_i(\mathbf{p}_{0Gi} - \mathbf{p}_{0i})$, and ${}^ia_{0i} = \mathbf{R}^0_i\mathbf{a}_{0i}$. It is noted that the variables without the front superscript are expressed in the base coordinate system.

The inertial force ${}^i\vec{\mathbf{F}}^i_0$ and moment ${}^i\vec{\mathbf{M}}^i_0$ acting on link i can then be expressed in the ith coordinate frame (about the gravitational center of link i) as follows:

$$ {}^i\vec{\mathbf{F}}^i_0 = m_i\,{}^i\vec{\mathbf{a}}_{0Gi} \tag{10} $$

$$ {}^i\vec{\mathbf{M}}^i_0 = {}^i\mathbf{I}_{0i}\,{}^i\dot{\vec{\omega}}_{0i} + {}^i\vec{\omega}_{0i} \times {}^i\mathbf{I}_{0i}({}^i\vec{\omega}_{0i}) \tag{11} $$

where $\ddot{\mathbf{p}}_{0Gi} = \mathbf{a}_{0Gi}$ is the translational acceleration of the gravity center G_i in the base coordinate system and ${}^i\mathbf{I}_{0i} = \mathbf{R}^0_i\mathbf{I}_{0i}\mathbf{R}^i_0$ is the "reflected" second order inertial moment, $\mathbf{I}_{0i}$ is the moment of inertia of link i about the gravitational center, and ${}^i\omega_{0i} = [0, 0, \Sigma^i_{k=2}\,\dot{\theta}_k]^T$.

Eqs. (4)–(11) represent (forward) difference equations with respect to the link number. They can be solved by starting from the first link, and proceeding toward the end-effector (the bucket), i.e., by setting $i = 1$, 2 and 3.

For the mathematical analysis, the links of the excavator are separated at the joints to form the free bodies (Fig. 3). Then, for each free body, such as link i, the forces are balanced and expressed in the ith coordinate system to obtain

$$ {}^i\vec{\mathbf{F}}_{(i-1)i} = {}^i\vec{\mathbf{F}}_{i(i+1)} + \sum_k {}^i\vec{\mathbf{F}}^{\,\mathrm{ext}}_k + {}^i\vec{\mathbf{F}}^i_0 \tag{12} $$

where ${}^i\vec{\mathbf{F}}_{(i-1)i}$ = force acting on link i from link $(i-1)$ and expressed in the ith coordinate frame. ${}^i\vec{\mathbf{F}}_k^{\text{ext}}$ signifies an external force (e.g., the piston force of a hydraulic actuator) acting on link i.

$$
\begin{aligned}
{}^i\vec{\mathbf{M}}_{(i-1)i} &= {}^i\vec{\mathbf{M}}_{i(i+1)} + ({}^i\vec{\mathbf{p}}_{0i} - {}^i\vec{\mathbf{p}}_{0Gi}) \times {}^i\vec{\mathbf{F}}_{i(i+1)} \\
&\quad + [{}^i\vec{\mathbf{p}}_{0Gi} - {}^i\vec{\mathbf{p}}_{0(i-1)}] \times {}^i\vec{\mathbf{F}}_{(i-1)i} + {}^i\vec{\mathbf{M}}_0^i
\end{aligned} \tag{13}
$$

where ${}^i\vec{\mathbf{M}}_{(i-1)i}$ is the moment acting on link i from link $(i-1)$ and expressed in the ith coordinate frame. Eqs. (12) and (13) can be combined to obtain

$$
\begin{aligned}
{}^i\vec{\mathbf{M}}_{(i-1)i} &= {}^i\vec{\mathbf{M}}_{i(i-1)} + [{}^i\vec{\mathbf{p}}_{0i} - {}^i\vec{\mathbf{p}}_{0(i-1)}] \times {}^i\vec{\mathbf{F}}_{i(i-1)} \\
&\quad + [{}^i\vec{\mathbf{p}}_{0Gi} - {}^i\vec{\mathbf{p}}_{0(i-1)}] \times {}^i\vec{\mathbf{F}}_0^i + [{}^i\vec{\mathbf{p}}_{0Gi} - {}^i\vec{\mathbf{p}}_{0(i-1)}] \\
&\quad \times \sum_k {}^i\vec{\mathbf{F}}_k^{\text{exp}} + {}^i\vec{\mathbf{M}}_0^i
\end{aligned} \tag{14}
$$

Eqs. (12) and (14) can be solved backward by starting from the end-effector ($i = 4$) and proceeding toward the base.

The dynamics of link i of the excavator are governed by (10) and (12), and (11) and (14), which represent Newton's and Euler's equations. These equations for the entire excavator are presented in detail in Appendix II.

By combining the equations of all links, i.e., (51), (59), and (79), the dynamic model for the motion of the excavator can be expressed concisely as follows:

$$
\mathbf{D}(\boldsymbol{\theta})\ddot{\boldsymbol{\theta}} + \mathbf{C}(\boldsymbol{\theta}, \dot{\boldsymbol{\theta}})\dot{\boldsymbol{\theta}} + \mathbf{G}(\boldsymbol{\theta}) + \mathbf{B}(\dot{\boldsymbol{\theta}}) = \boldsymbol{\Gamma}(\boldsymbol{\theta})\mathbf{F} - \mathbf{F}_{\text{load}}(F_t, F_n) \tag{15}
$$

where $\boldsymbol{\theta} = [\theta_1\ \theta_2\ \theta_3\ \theta_4]^T$ and θ_i, $i = 1, 2, 3, 4$ represents the shaft angle of joint i. The (4×4) matrix $\boldsymbol{\Gamma}(\boldsymbol{\theta})$ is a function of the moment arms; vector $\mathbf{F} = [F_b\ F_{BE}\ F_{FJ}\ F_{JK}]^T$ specifies the forces of the hydraulic actuators which produce the torques acting on the joint shafts; the first component $F_b \equiv 0$ since the first joint is not moved. Term $\mathbf{F}_{\text{load}}$ is determined by the forces F_n and F_t acting on the bucket due to soil and bucket interaction as shown in Fig. 2 and presented in Appendix III. Vector $\mathbf{G}(\boldsymbol{\theta})$ describes the gravity, $\mathbf{C}(\boldsymbol{\theta}, \dot{\boldsymbol{\theta}})\dot{\boldsymbol{\theta}}$ is determined by the Coriolis and centripetal effects, $\mathbf{D}(\boldsymbol{\theta})$ is the (pseudo) inertial matrix, and $\mathbf{B}(\dot{\boldsymbol{\theta}})$ signifies friction.

Specifically, $\mathbf{G}(\boldsymbol{\theta})$, $\mathbf{C}(\boldsymbol{\theta}, \dot{\boldsymbol{\theta}})$ and $\mathbf{D}(\boldsymbol{\theta})$ are given by the following expressions:

$$
\mathbf{G}(\boldsymbol{\theta}) = [G_1\ G_2\ G_3\ G_4]^T \tag{16}
$$

$$
\mathbf{C}(\boldsymbol{\theta}, \dot{\boldsymbol{\theta}})\dot{\boldsymbol{\theta}} = \begin{bmatrix} C_{11} & C_{12} & C_{13} & C_{14} \\ C_{21} & C_{22} & C_{23} & C_{24} \\ C_{31} & C_{32} & C_{33} & C_{34} \\ C_{41} & C_{42} & C_{43} & C_{44} \end{bmatrix} \begin{pmatrix} \dot{\theta}_1 \\ \dot{\theta}_2 \\ \dot{\theta}_3 \\ \dot{\theta}_4 \end{pmatrix} \tag{17}
$$

where in $G_2 = -m_4 g[l_2 c_2 + l_3 c_{23} + L_{03G4}\cos(\theta_{234} + \sigma_4)] - m_3 g[l_2 c_2 + L_{02G3}\cos(\theta_{23} + \sigma_5)] - m_2 g L_{01G2}\cos(\theta_2 + \sigma_9)$; $G_3 = -m_4 g[l_3 c_{23} + L_{03G4}\cos(\theta_{234} + \sigma_4)] - m_3 g L_{02G3}\cos(\theta_{23} + \sigma_5)$; $G_4 = -m_4 g L_{03G4}\cos(\theta_{234} + \sigma_4)$; $C_{22} = -2[d' + k\sin(\theta_{34} + \sigma_4)]\dot{\theta}_3 - 2[k\sin(\theta_{34} + \sigma_4) + n\sin(\theta_4 + \sigma_4)]\dot{\theta}_4$, and $d' = m_3 l_2 L_{02G3}\sin(\theta_3 + \sigma_5) + m_4 l_2 l_3 S_3$, $k = m_4 l_2 L_{03G4}$, $n = m_4 l_3 L_{03G4}$; $C_{23} = -[d' + k\sin(\theta_{34} + \sigma_4)]\dot{\theta}_3 - 2[k\sin(\theta_{34} + \sigma_4) + n\sin(\theta_4 + \sigma_4)]\dot{\theta}_4$; $C_{24} = -[k\sin(\theta_{34} + \sigma_4) + n\sin(\theta_4 + \sigma_4)]\dot{\theta}_4$; $C_{32} = [d' + k\sin(\theta_{34} + \sigma_4)]\dot{\theta}_2 - [n\sin(\theta_4 + \sigma_4)]\dot{\theta}_4$; $C_{33} = -[n\sin(\theta_4 + \sigma_4)]\dot{\theta}_4$; $C_{34} = -[n\sin(\theta_4 + \sigma_4)](\dot{\theta}_2 + \dot{\theta}_3 + \dot{\theta}_4)$; $C_{42} = [k\sin(\theta_{34} + \sigma_4) + n\sin(\theta_4 + \sigma_4)]\dot{\theta}_2 - [n\sin(\theta_4 + \sigma_4)]\dot{\theta}_3$; $C_{43} = [n\sin(\theta_4 + \sigma_4)](\dot{\theta}_2 + \dot{\theta}_3)$; $C_{44} = 0$. Moreover

$$
\mathbf{D}(\boldsymbol{\theta}) = \begin{bmatrix} D_{11} & D_{12} & D_{13} & D_{14} \\ D_{21} & D_{22} & D_{23} & D_{24} \\ D_{31} & D_{32} & D_{33} & D_{34} \\ D_{41} & D_{42} & D_{43} & c \end{bmatrix} \tag{18}
$$

where $D_{22} = \bar{a}_1 + 2d + 2n\cos(\theta_4 + \sigma_4) + 2k\cos(\theta_{34} + \sigma_4)$; $D_{23} = D_{32} = \bar{a}_2 + d + 2n\cos(\theta_4 + \sigma_4) + k\cos(\theta_{34} + \sigma_4)$; $D_{24} = D_{42} = c + n\cos(\theta_4 + \sigma_4) + k\cos(\theta_{34} + \sigma_4)$; $D_{33} = \bar{a}_2 + 2n\cos(\theta_4 + \sigma_4)$; $D_{34} = D_{43} = c + n\cos(\theta_4 + \sigma_4)$; $\bar{a}_1 = a + b + c$; $\bar{a}_2 = b + c$; $a = m_2 L_{01G2}^2 + I_{02} + (m_3 + m_4)l_2^2$; $b = m_3 L_{02G3}^2 + I_{03} + m_4 l_3^2$; $c = m_4 L_{03G4}^2 + I_{04}$; $d = m_3 l_2 L_{02G3}\cos(\theta_3 + \sigma_5) + m_4 l_2 l_3 c_3$; m_i and l_i = mass and length of link i, respectively; I_i = its second-order inertial moment about the rotational axis through the gravity center; $g = -9.81\ \text{m/s}^2$; $c_i = \cos\theta_i$; $c_{ij} = \cos(\theta_i + \theta_j)$; $c_{ijk} = \cos(\theta_i + \theta_j + \theta_k)$; and s_i, s_{ij}, s_{ijk} = corresponding expressions of the sin function.

$$
\boldsymbol{\Gamma}(\boldsymbol{\theta}) = \begin{bmatrix} \Gamma_{11} & \Gamma_{12} & \Gamma_{13} & \Gamma_{14} \\ 0 & \Gamma_{22} & \Gamma_{23} & \Gamma_{24} \\ 0 & 0 & \Gamma_{33} & \Gamma_{34} \\ 0 & 0 & 0 & \Gamma_{44} \end{bmatrix} \tag{19a}
$$

where the elements of $\boldsymbol{\Gamma}(\boldsymbol{\theta})$ are defined as

$$
\Gamma_{22} = L_{01B}\sin(\rho - \theta_2 - \sigma_{11});
$$

$$
\Gamma_{23} = L_{01I}\sin(\theta_3 + \sigma_{10} + \gamma_2) - l_2\sin(\theta_3 + \gamma_2) \tag{19b}
$$

$$
\begin{aligned}
\Gamma_{24} &= L_{0102}\sin(\gamma_1 + \theta_3) \\
&\quad - L_{0102}\sin(\varepsilon_4 + \theta_3)\left[\frac{\sin\gamma_1 - \cos\gamma_1\tan\varepsilon_4}{\sin(\theta_{23} - \varepsilon_5) + \tan\varepsilon_4\cos(\theta_{23} - \varepsilon_5)}\right] \\
&\quad - L_{0102}\sin(\gamma_2 - \varepsilon_5)\left[\frac{\cos\gamma_1\tan(\theta_{23} - \varepsilon_5) + \sin\gamma_1}{\cos\varepsilon_4\tan(\theta_{23} - \varepsilon_5) + \sin\varepsilon_4}\right]
\end{aligned} \tag{19c}
$$

$$
\begin{aligned}
\Gamma_{33} &= L_{02F}\sin(\sigma_8 - \gamma_2) - L_{cj}\sin(\gamma_2 - \sigma_7) \\
&\quad - L_{0203}\sin(\theta_{23} - \varepsilon_5)\left[\frac{\cos\gamma_1\tan(\theta_{23} - \varepsilon_5) + \sin\gamma_1}{\cos\varepsilon_4\tan(\theta_{23} - \varepsilon_5) + \sin\varepsilon_4}\right]
\end{aligned} \tag{19d}
$$

$$
\begin{aligned}
\Gamma_{34} &= -L_{02L}\sin(\varepsilon_4 - \sigma_6)\left[\frac{\tan(\theta_{23} - \varepsilon_5)\cos\gamma_1 + \sin\gamma_1}{\sin\varepsilon_4 + \cos\varepsilon_4\tan(\theta_{23} - \varepsilon_5)}\right] \\
&\quad + L_{02J}\sin(\sigma_7 - \gamma_1) + l_3\sin(\varepsilon_5 - \theta_{23}) \\
&\quad \cdot\left[\frac{\tan\varepsilon_4\cos\gamma_1 - \sin\gamma_1}{\sin(\theta_{23} - \varepsilon_5) - \tan\varepsilon_4\cos(\theta_{23} - \varepsilon_5)}\right]
\end{aligned} \tag{19e}
$$

$$
\begin{aligned}
\Gamma_{44} &= L_{03P}\sin[\varepsilon_5 - (\angle_{PO_3O_4} - \theta_{234})] \\
&\quad \cdot\left[\frac{\tan\varepsilon_4\cos\gamma_1 - \sin\gamma_1}{\sin(\theta_{23} - \varepsilon_5) - \tan\varepsilon_4\cos(\theta_{23} - \varepsilon_5)}\right]
\end{aligned} \tag{19f}
$$

Moreover, the loading torque $\mathbf{F}_{\text{load}}$ in (15) is

$$
\mathbf{F}_{\text{load}}(\mathbf{F}_t, \mathbf{F}_n) = \begin{pmatrix} F_1 \\ a_2[F_t\sin(\theta_2 - \theta_{dg}) - F_n\cos(\theta_2 - \theta_{dg})] \\ a_3[F_t\sin(\theta_{23} - \theta_{dg}) - F_n\cos(\theta_{23} - \theta_{dg})] \\ a_4(-F_t\sin\theta_b + F_n\cos\theta_b) \end{pmatrix} \tag{20}
$$

Elements D_{1i}, D_{i1}, C_{1i}, C_{i1}, Γ_{1i}, $i = 1, 2, 3, 4$, G_1, and F_1 are not specified here because the joint variable θ_1 is not changed during the digging operation.

One may observe that the inertia matrix $\mathbf{D}(\boldsymbol{\theta})$ is symmetric and positive definite (due to the kinetic energy expression for the excavator motion) as in the model of robotic manipulators.

It should be noted that the model in (15) differs in many respects from the one given in Vähä and Skibniewski [(1993) their equation 4]. Ignoring the obvious typos in their model, the main difference is in the expression $\boldsymbol{\Gamma}(\boldsymbol{\theta})$ of our (15) and (19), which contains also nonzero off-diagonal terms contrary

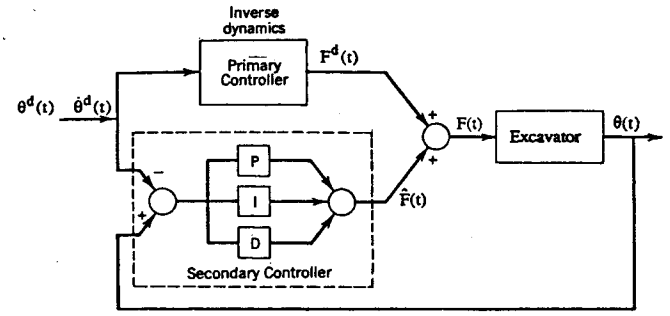

FIG. 4. Control Architecture

to Vähä and Skibniewski (1993). It appears that it is assumed implicitly in Vähä and Skibniewski (1993) that the gravity centers of the links are on the line joining the endpoints of the links; this assumption in most cases is not valid. The model presented here corrects several of the shortcomings of the foregoing paper.

SIMULATIONS

A simulation study on a (hypothetical) excavator was performed in C language programming environment (C++ 4.0, Borland, Scotts Valley, Calif., 1993; MathCad 3.1, MathSoft, 1992). During a digging operation, soil is removed by a plowing action. The depth of the bucket edge, i.e., the cut depth is determined so that the bucket is full at the end of the stroke, and that the excavating forces do not unduly impede the progress of the bucket.

A desired trajectory is first designed in the Cartesian space. Using the inverse kinematic equations of the excavator (Koivo 1994), the desired joint positions are calculated. The joint positions are used to generate the joint velocities and accelerations with software.

To make the bucket of the excavator track the desired trajectory, the control system shown in Fig. 4 is designed. As Fig. 4 indicates, the primary controller generates the generalized torques to be applied to the system, producing the desired motion under ideal conditions. It is specified by the inverse dynamics of the excavator, (15). A secondary controller in Fig. 4 is then designed to compensate for deviations of the actual motion from the desired trajectory. In fact, the gains of the controller can be determined experimentally so that the a specified overshoot and settling time in the step responses (Koivo 1989) are obtained.

The excavator motion was simulated using (15) with the numerical values given in Appendix IV. The primary controller was calculated using 10% offset in the values of the masses. The secondary controller $\hat{\mathbf{F}}(t)$ was chosen as a PD-controller operating on the tracking error $e(t)$ and a P-controller on the force error

$$\hat{\mathbf{F}}(t) = \mathbf{K}_P\mathbf{e}(t) + \mathbf{K}_D\dot{\mathbf{e}}(t) + \mathbf{K}_I[\mathbf{F}_{\text{load}}(t) - \mathbf{F}^d_{\text{load}}(t)] \quad (21)$$

where $\mathbf{e}(t) = \boldsymbol{\theta}(t) - \boldsymbol{\theta}^d(t)$; force $\mathbf{F}^d_{\text{load}}(t)$ = desired force exerted by the bucket on the soil; and $\mathbf{K}_P$, $\mathbf{K}_D$, and $\mathbf{K}_I$ = controller gains that are adjusted experimentally for 10% overshoot and 0.1 s settling time in the step responses.

The simulation results are presented in Fig. 5. The mean squared tracking error of the three joints is $8.095\ 10^{-4}$ rad. The simulations illustrate that the controller performs very well during the free (gross) motion and the constrained motion (digging).

CONCLUSION

A dynamic model for an excavator performing a digging operation is presented in Newton-Euler's formulation. The

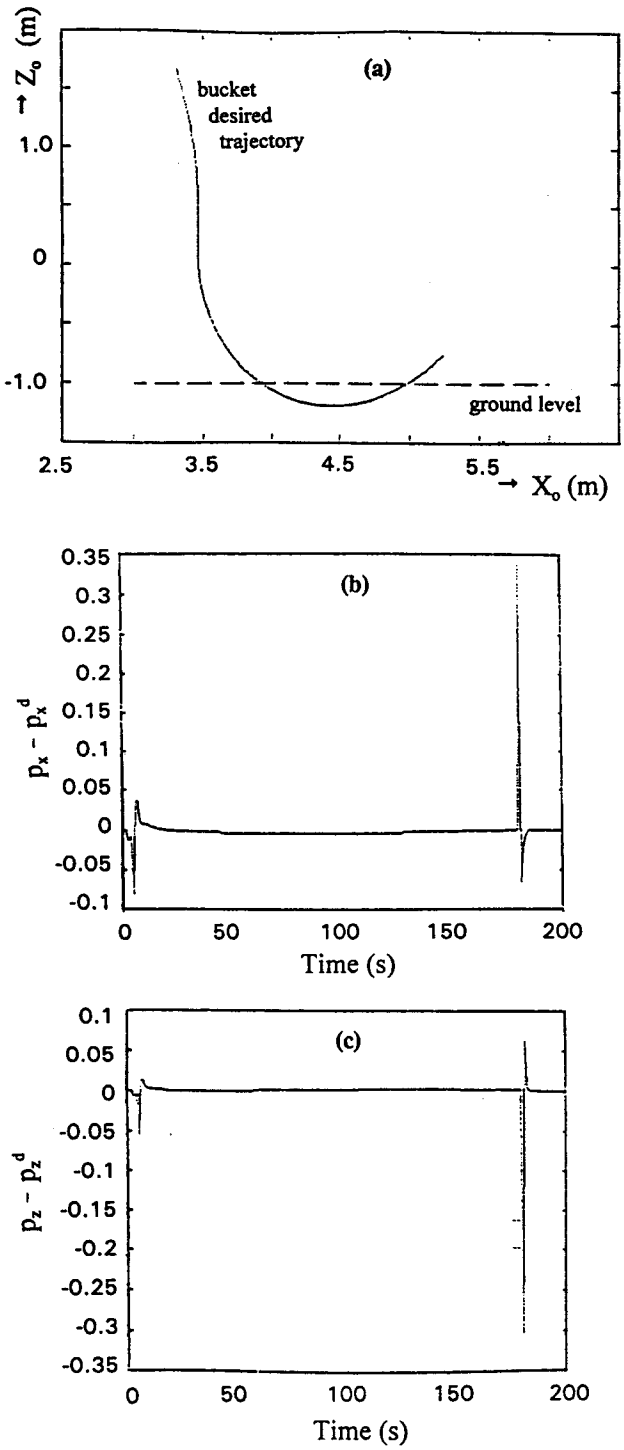

FIG. 5. Bucket Trajectories: (a) Desired Trajectory; (b) *x*-Coordinate Error of Bucket Position versus Time; (c) *z*-Coordinate Error of Bucket Position versus Time

equations of motion are derived by first presenting the velocities and accelerations of the gravity centers of the links as forward difference equations relative to the link number. Then, the equations for the forces and torques acting on the links are described by backward difference equations relative to the link number. By combining the equations, the dynamical model for the joint variables is obtained. It is in a form similar to the equations of motion of robotic manipulators.

The model derived systematically corrects several inadequacies that appear in previously published (Vähä and Skibniewski 1993) model of excavators. Simulations that illustrate

the use of the proposed dynamical model and the performance of the proposed control scheme are presented.

The dynamical model obtained can be used as the basis for automating the operations of excavators. It can be accomplished by designing a control scheme so that the entire system can operate in an autonomous mode. The approach presented can equally well be applied to the operations of backhoes.

ACKNOWLEDGMENTS

The writers would like to express their appreciation to Dr. P. Vähä of the Technical Research Center of Finland (Oulu, Finland) for interesting discussions on the subject. This work was partly supported by the NATO Scientific Affairs Division, NATO 5-2-05/CRG No. 910661 437/94/AHJ-513 and by Alexander von Humboldt Foundation Senior Research Award.

APPENDIX I. FORWARD EQUATIONS FOR VELOCITIES AND ACCELERATIONS

It will be assumed that the excavator is operating on the plane determined by the centerlines of links 2, 3, and 4 (the bucket). Thus, link 1 (the base of the carrier) is not moved during the digging operation, which is usually the case. To determine the equations of motion for links 2, 3, and 4 of the excavator, the equations for the rotational and translational velocities of the links are first obtained.

For link 2, the rotational and translational velocities expressed in the second coordinate frame are

$$ {}^2\boldsymbol{\omega}_{02} = [0,\ 0,\ \dot{\theta}_2]^T \tag{22} $$

$$ {}^2\mathbf{v}_{02} = [0,\ L_{O_1O_2}\dot{\theta}_2,\ 0]^T \tag{23} $$

$$ {}^2\boldsymbol{\alpha}_{02} = {}^2\dot{\boldsymbol{\omega}}_{02} = [0,\ 0,\ \ddot{\theta}_2]^T \tag{24} $$

$$ {}^2\mathbf{a}_{02} = [-L_{O_1O_2}\dot{\theta}_2^2,\ L_{O_1O_2}\ddot{\theta}_2,\ 0]^T \tag{25} $$

$$ {}^2\mathbf{v}_{0G_2} = [-L_{O_2G_2}\dot{\theta}_2 \sin(\sigma_1),\ -L_{O_2G_2}\dot{\theta}_2 \cos(\sigma_1) + L_{O_1O_2}\dot{\theta}_2,\ 0]^T \tag{26} $$

where $\sigma_1 = \angle G_2O_2O_1$.

$$ {}^2\mathbf{a}_{0G_2} = \begin{pmatrix} -L_{O_2G_2}\ddot{\theta}_2 \sin(\sigma_1) + L_{O_2G_2}\dot{\theta}_2^2 \cos(\sigma_1) - L_{O_1O_2}\dot{\theta}_2^2 \\ -L_{O_2G_2}\ddot{\theta}_2 \cos(\sigma_1) - L_{O_2G_2}\dot{\theta}_2^2 \sin(\sigma_1) + L_{O_1O_2}\ddot{\theta}_2 \\ 0 \end{pmatrix} \tag{27} $$

Then, by (10) and (11),

$$ {}^2\mathbf{F}_0^2 = \begin{bmatrix} -L_{O_2G_2} m_2\ddot{\theta}_2 \sin(\sigma_1) + m_2\dot{\theta}_2^2[-L_{O_1O_2} + L_{O_2G_2}\cos(\sigma_1)] \\ \quad + m_2 g s_2 \\ m_2\ddot{\theta}_2[L_{O_1O_2} - L_{O_2G_2}\cos(\sigma_1)] - m_2\dot{\theta}_2^2 L_{O_2G_2}\sin(\sigma_1) \\ \quad + m_2 g c_2 \\ 0 \end{bmatrix} \tag{28} $$

$$ {}^2\mathbf{M}_0^2 = [0,\ 0,\ I_{02}\ddot{\theta}_2]^T \tag{29} $$

where $\mathbf{I}_{02}$ = second (inertial) moment about the rotational axis through the gravity center of link 2. Eqs. (26)–(29) establish the velocity, acceleration vectors, the inertial force and moment for link 2.

For link 3, the corresponding equations are written

$$ {}^3\boldsymbol{\omega}_{03} = [0,\ 0,\ \dot{\theta}_2 + \dot{\theta}_3]^T \tag{30} $$

$$ {}^3\mathbf{v}_{03} = [L_{O_1O_2}\dot{\theta}_2 s_3,\ L_{O_1O_2}\dot{\theta}_2 c_3 + (\dot{\theta}_2 + \dot{\theta}_3)L_{O_2G_3},\ 0]^T \tag{31} $$

$$ {}^3\boldsymbol{\alpha}_{03} = {}^3\dot{\boldsymbol{\omega}}_{03} = [0,\ 0,\ \ddot{\theta}_2 + \ddot{\theta}_3]^T \tag{32} $$

$$ {}^3\mathbf{a}_{03} = \begin{pmatrix} L_{O_1O_2}\ddot{\theta}_2 s_3 - L_{O_1O_2}\dot{\theta}_2^2 c_3 - (\dot{\theta}_2 + \dot{\theta}_3)^2 L_{O_2O_3} \\ L_{O_1O_2}\dot{\theta}_2^2 s_3 + L_{O_1O_2}\ddot{\theta}_2 c_3 + (\ddot{\theta}_2 + \ddot{\theta}_3)L_{O_2O_3} \\ 0 \end{pmatrix} \tag{33} $$

$$ {}^3\mathbf{v}_{0G_3} = \begin{pmatrix} L_{O_1O_2}\dot{\theta}_2 s_3 - (\dot{\theta}_2 + \dot{\theta}_3)L_{G_3O_3}\sin(\sigma_2) \\ L_{O_1O_2}\dot{\theta}_2 c_3 + (\dot{\theta}_2 + \dot{\theta}_3)L_{O_2O_3} - (\dot{\theta}_2 + \dot{\theta}_3)L_{G_3O_3}\cos(\sigma_2) \\ 0 \end{pmatrix} \tag{34} $$

where $\sigma_2 = \angle G_3O_3O_2$

$$ {}^3\mathbf{a}_{0G_3} = \begin{bmatrix} L_{O_1O_2}\ddot{\theta}_2 s_3 - L_{O_1O_2}\dot{\theta}_2^2 c_3 - L_{O_2O_3}(\dot{\theta}_2 + \dot{\theta}_3)^2 \\ \quad - (\ddot{\theta}_2 + \ddot{\theta}_3)L_{G_3O_3}\sin(\sigma_2) + L_{G_3O_3}\cos(\sigma_2)(\dot{\theta}_2 + \dot{\theta}_3)^2 \\ L_{O_1O_2}s_3\dot{\theta}_2^2 + L_{O_1O_2}c_3\ddot{\theta}_2 + L_{O_2O_3}(\ddot{\theta}_2 + \ddot{\theta}_3) \\ \quad - L_{G_3O_3}\cos(\sigma_2)(\ddot{\theta}_2 + \ddot{\theta}_3) - L_{G_3O_3}\sin(\sigma_2)(\dot{\theta}_2 + \dot{\theta}_3)^2 \\ 0 \end{bmatrix} \tag{35} $$

Then (10) and (11) for $i = 3$ yield

$$ {}^3\mathbf{F}_0^3 = m_3\,{}^3\mathbf{a}_{0G_3} + m_3\mathbf{g}_3 \tag{36} $$

$$ {}^3\mathbf{M}_0^3 = [0,\ 0,\ I_{03}(\ddot{\theta}_2 + \ddot{\theta}_3)]^T \tag{37} $$

where $\mathbf{g}_3 = [g s_{23},\ g c_{23},\ 0]^T$; and I_{03} = second (inertial) moment about the rotational axis through the center of the gravity of link 3.

Eqs. (34)–(37) describe the velocity and acceleration vectors, and the inertial force and moment vectors for link 3.

For link 4 (bucket), the forward equations are written when $i = 4$

$$ {}^4\boldsymbol{\omega}_{04} = [0,\ 0,\ \dot{\theta}_2 + \dot{\theta}_3 + \dot{\theta}_4]^T \tag{38} $$

$$ {}^4\mathbf{v}_{04} = \begin{pmatrix} L_{O_1O_2}s_{34}\dot{\theta}_2 + L_{O_2O_3}s_4(\dot{\theta}_2 + \dot{\theta}_3) \\ L_{O_1O_2}\dot{\theta}_2 c_{34} + L_{O_2O_3}c_4(\dot{\theta}_2 + \dot{\theta}_3) + L_{O_3O_4}(\dot{\theta}_2 + \dot{\theta}_3 + \dot{\theta}_4) \\ 0 \end{pmatrix} \tag{39} $$

$$ {}^4\boldsymbol{\alpha}_{04} = [0,\ 0,\ \ddot{\theta}_2 + \ddot{\theta}_3 + \ddot{\theta}_4]^T \tag{40} $$

$$ {}^4\mathbf{a}_{04} = \begin{bmatrix} -L_{O_1O_2}c_{34}\dot{\theta}_2^2 + L_{O_1O_2}s_{34}\ddot{\theta}_2 - L_{O_2O_3}c_4(\dot{\theta}_2 + \dot{\theta}_3)^2 \\ \quad - L_{O_3O_4}(\dot{\theta}_2 + \dot{\theta}_3 + \dot{\theta}_4)^2 + L_{O_2O_3}s_4(\ddot{\theta}_2 + \ddot{\theta}_3) \\ L_{O_1O_2}s_{34}\dot{\theta}_2^2 + L_{O_1O_2}c_{34}\ddot{\theta}_2 + L_{O_2O_3}s_4(\dot{\theta}_2 + \dot{\theta}_3)^2 \\ \quad + L_{O_2O_3}c_4(\ddot{\theta}_2 + \ddot{\theta}_3) + L_{O_3O_4}(\ddot{\theta}_2 + \ddot{\theta}_3 + \ddot{\theta}_4) \\ 0 \end{bmatrix} \tag{41} $$

$$ {}^4\mathbf{v}_{0G_4} = \begin{bmatrix} L_{O_1O_2}s_{34}\dot{\theta}_2 + L_{O_2O_3}s_4(\dot{\theta}_2 + \dot{\theta}_3) \\ \quad - L_{G_4O_4}\sin(\sigma_3)(\dot{\theta}_2 + \dot{\theta}_3 + \dot{\theta}_4) \\ L_{O_1O_2}c_{34}\dot{\theta}_2 + L_{O_2O_3}c_4(\dot{\theta}_2 + \dot{\theta}_3) + L_{O_3O_4}(\dot{\theta}_2 + \dot{\theta}_3 + \dot{\theta}_4) \\ \quad - L_{G_4O_4}\cos(\sigma_3)(\dot{\theta}_2 + \dot{\theta}_3 + \dot{\theta}_4) \\ 0 \end{bmatrix} \tag{42} $$

where $\sigma_3 = \angle G_4O_4O_3$. By writing ${}^4\mathbf{a}_{04} = [{}^4a_{04x}\ {}^4a_{04y}\ {}^4a_{04z}]^T$, one obtains

$$ {}^4\mathbf{a}_{0G4} = \begin{bmatrix} {}^4a_{04x} - L_{O4G4}\sin(\sigma_3)(\ddot{\theta}_2 + \ddot{\theta}_3 + \ddot{\theta}_4) \\ \quad + L_{O4G4}\cos(\sigma_3)(\dot{\theta}_2 + \dot{\theta}_3 + \dot{\theta}_4)^2 \\ {}^4a_{04y} - L_{O4G4}\cos(\sigma_3)(\ddot{\theta}_2 + \ddot{\theta}_3 + \ddot{\theta}_4) \\ \quad - L_{O4G4}\sin(\sigma_3)(\dot{\theta}_2 + \dot{\theta}_3 + \dot{\theta}_4)^2 \\ 0 \end{bmatrix} \quad (43) $$

By assuming that the mass of the bucket stays constant during the motion, it then follows that the inertial force and moments are

$$ {}^4\mathbf{F}_0^4 = m_4\,{}^4\mathbf{a}_{0G4} + m_4\mathbf{g}_4 \quad (44) $$

$$ {}^4\mathbf{M}_0^4 = [0,\ 0,\ I_{04}(\ddot{\theta}_2 + \ddot{\theta}_3 + \ddot{\theta}_4)]^T \quad (45) $$

where $\mathbf{g}_4 = [gs_{234}\ gc_{234}\ 0]^T$.

Eqs. (42)–(45) specify the velocity and acceleration vectors, as well as the force and inertial moment vectors for link 4.

APPENDIX II. EQUATIONS OF MOTION FOR EACH LINK

For each free body i, $i = 2, 3, 4$ in Figs. 3(a), (b), and (c), the force and moment equations are determined by starting from the end-effector, i.e., from the last link $i = 4$, and proceeding toward the base. The general equations (12) and (14) are next applied to each link.

For link $i = 4$, (12) is first written as column vectors in the first-coordinate system

$$ \mathbf{F}_{34} = \mathbf{F}_{45} - \mathbf{F}_{PK} - \mathbf{F}_0^4 \quad (46) $$

where $\mathbf{F}_{34} = [F_{34x},\ 0,\ F_{34z}]^T$ in the zeroth coordinate frame.

The specific expressions of the variables in (46) are

$$ \mathbf{F}_{45} = [F_t\cos\theta_{dg} - F_n\sin\theta_{dg},\ 0,\ F_t\sin\theta_{dg} + F_n\cos\theta_{dg}]^T \quad (47) $$

and F_t and F_n = tangential and normal reaction forces, respectively, acting between the bucket and soil.

$$ \mathbf{F}_{PK} = [F_{PK}\cos\varepsilon_5,\ 0,\ F_{PK}\sin\varepsilon_5]^T \quad (48) $$

$$ \mathbf{F}_0^4 = [F_{0x}^4,\ 0,\ F_{0z}^4]^T \quad (49) $$

where ε_5 = angle that $\overline{PK}$ makes with the line that is parallel with the positive X_1-axis; it can be measured by an encoder, or a trigonometric relationship can be established for ε_5 in terms of θ_2, θ_3, θ_4 and the structural link-parameters. Also, $\mathbf{F}_0^4 = \mathbf{R}_0^4({}^4\mathbf{F}_0^4)$ where $\mathbf{R}_0^4 = (\mathbf{A}_0^4)_R$ is the rotation submatrix in the homogeneous transformation matrix $\mathbf{A}_0^4$, and ${}^4\mathbf{F}_0^4$ is specified in (44).

Eqs. (46) and (13) can be combined and the result expressed in the fourth coordinate frame to obtain [(13) with $i = 4$]

$$ {}^4\vec{\mathbf{M}}_{34} = {}^4\vec{\mathbf{M}}_{45} + ({}^4\vec{\mathbf{p}}_{0P} - {}^4\vec{\mathbf{p}}_{0G4}) \times {}^4\vec{\mathbf{F}}_{PK} - ({}^4\vec{\mathbf{p}}_{04} - {}^4\vec{\mathbf{p}}_{0G4}) \times {}^4\vec{\mathbf{F}}_{45} + ({}^4\vec{\mathbf{p}}_{03} - {}^4\vec{\mathbf{p}}_{0G4}) \times {}^4\vec{\mathbf{F}}_{34} + {}^4\vec{\mathbf{M}}_0^4 \quad (50) $$

Force ${}^4\vec{\mathbf{F}}_{34}$ is obtained from (46) after it is expressed in the fourth coordinate frame. Thus

$$ {}_s^4\vec{\mathbf{M}}_{34} = {}^4\vec{\mathbf{M}}_{45} - ({}^4\vec{\mathbf{p}}_{04} - {}^4\vec{\mathbf{p}}_{03}) \times {}^4\vec{\mathbf{F}}_{45} + ({}^4\vec{\mathbf{p}}_{0G4} - {}^4\vec{\mathbf{p}}_{03}) \times {}^4\vec{\mathbf{F}}_0^4 + {}^4\vec{\mathbf{M}}_0^4 \quad (51) $$

$$ {}_s^4\vec{\mathbf{M}}_{34} = {}^4\vec{\mathbf{M}}_{34} - ({}^4\vec{\mathbf{p}}_{0P} - {}^4\vec{\mathbf{p}}_{03}) \times {}^4\vec{\mathbf{F}}_{PK} \quad (52) $$

where moment ${}^4\mathbf{M}_{45}$ about the bucket edge axis is zero. By setting $\theta_2 + \theta_3 + \theta_4 - \pi - \theta_{dg} = \theta_b$ in (47), one has

$$ {}^4\vec{\mathbf{F}}_{45} = [-F_t\cos\theta_b - F_n\sin\theta_b,\ F_t\sin\theta_b - F_n\cos\theta_b,\ 0]^T \quad (53) $$

$$ ({}^4\vec{\mathbf{p}}_{04} - {}^4\vec{\mathbf{p}}_{03}) \times {}^4\vec{\mathbf{F}}_{45} = L_{O3O4}(F_t\sin\theta_b - F_n\cos\theta_b)\vec{\mathbf{k}}_{z4} \quad (54) $$

$$ ({}^4\vec{\mathbf{p}}_{0P} - {}^4\vec{\mathbf{p}}_{03}) \times {}^4\vec{\mathbf{F}}_{PK} = F_{PK}L_{O3P}(\sin\xi)\vec{\mathbf{k}}_{z4} \quad (55) $$

where $\vec{\mathbf{k}}_{z4}$ = the unit vector in the z_4-direction, $\xi = \varepsilon_5 - (\angle PO_3O_4 + \varepsilon_5 - \theta_{234})$ and $\theta_{234} = \theta_2 + \theta_3 + \theta_4$. One observes that vector

$$ {}^4\mathbf{p}_{0G4} - {}^4\mathbf{p}_{03} = [L_{O3G4}\cos\sigma_4,\ L_{O3G4}\sin\sigma_4,\ 0]^T \quad (56) $$

emanates from point G_4 and that $\sigma_4 = \angle G_4O_3O_4$.

Since ${}^4\mathbf{F}_0^4$ and ${}^4\mathbf{M}_0^4$ are given by (44) and (45), respectively, all terms in (51) are specified. Thus, moment ${}^4\mathbf{M}_{34}$ can be calculated. Since all joint moments are about the joint axes, which are parallel, the superscripts in front of the moments and the unit vectors on the z_i-axis, $i = 1, 2, 3, 4$, are omitted in the sequel.

For link 3 ($i = 3$), (12) and (14) assume the following forms:

$$ {}^3\vec{\mathbf{F}}_{23} = {}^3\vec{\mathbf{F}}_{34} - {}^3\vec{\mathbf{F}}_{LK} - {}^3\vec{\mathbf{F}}_{JK} - {}^3\vec{\mathbf{F}}_{FI} - {}^3\vec{\mathbf{F}}_0^3 \quad (57) $$

$$ \vec{\mathbf{M}}_{23} = \vec{\mathbf{M}}_{34} - ({}^3\vec{\mathbf{p}}_{03} - {}^3\vec{\mathbf{p}}_{0G3}) \times {}^3\vec{\mathbf{F}}_{34} + ({}^3\vec{\mathbf{p}}_{02} - {}^3\vec{\mathbf{p}}_{0G3}) \times {}^3\vec{\mathbf{F}}_{23} + \vec{\mathbf{M}}_0^3 + ({}^3\vec{\mathbf{p}}_{0L} - {}^3\vec{\mathbf{p}}_{0G3}) \times \vec{\mathbf{F}}_{LK} + ({}^3\vec{\mathbf{p}}_{0J} - {}^3\vec{\mathbf{p}}_{0G3}) \times {}^3\vec{\mathbf{F}}_{JK} + ({}^3\vec{\mathbf{p}}_{0F} - {}^3\vec{\mathbf{p}}_{0G3}) \times {}^3\vec{\mathbf{F}}_{FI} \quad (58) $$

By combining (57) and (58), one has

$$ {}_s\vec{\mathbf{M}}_{23} = \vec{\mathbf{M}}_{23} - ({}^3\vec{\mathbf{p}}_{0L} - {}^3\vec{\mathbf{p}}_{02}) \times {}^3\vec{\mathbf{F}}_{LK} - ({}^3\vec{\mathbf{p}}_{0J} - {}^3\vec{\mathbf{p}}_{02}) \times {}^3\vec{\mathbf{F}}_{JK} - ({}^3\vec{\mathbf{p}}_{0F} - {}^3\vec{\mathbf{p}}_{02}) \times {}^3\vec{\mathbf{F}}_{FI} - ({}^3\vec{\mathbf{p}}_{03} - {}^3\vec{\mathbf{p}}_{02}) \times {}^3\vec{\mathbf{F}}_{PK} \quad (59) $$

$$ {}_s\vec{\mathbf{M}}_{23} = \vec{\mathbf{M}}_{34} - ({}^3\vec{\mathbf{p}}_{03} - {}^3\vec{\mathbf{p}}_{02}) \times {}_r^3\vec{\mathbf{F}}_{34} + ({}^3\vec{\mathbf{p}}_{0G3} - {}^3\vec{\mathbf{p}}_{02}) \times {}^3\vec{\mathbf{F}}_0^3 + \vec{\mathbf{M}}_0^3 \quad (60) $$

where ${}_r^3\vec{\mathbf{F}}_{34} = {}^3\vec{\mathbf{F}}_{34} + {}^3\vec{\mathbf{F}}_{PK} = {}^3\vec{\mathbf{F}}_{45} - {}^3\vec{\mathbf{F}}_0^4$. Moment $\vec{\mathbf{M}}_{34}$ is given in (51) where ${}^4\vec{\mathbf{M}}_{34} = \vec{\mathbf{M}}_{34}$. Moreover,

$$ ({}^3\vec{\mathbf{p}}_{03} - {}^3\vec{\mathbf{p}}_{02}) \times {}_r^3\vec{\mathbf{F}}_{34} = L_{O2O3}({}_r^3F_{34y})\vec{\mathbf{k}}_z = L_{O2O3}[-F_t\sin(\theta_{23} - \theta_{dg}) + F_n\cos(\theta_{23} - \theta_{dg}) + {}^3F_{0y}^4]\vec{\mathbf{k}}_z \quad (61) $$

$$ {}^3\mathbf{p}_{0G3} - {}^3\mathbf{p}_{02} = [L_{O2G3}\cos\sigma_5,\ L_{O2G3}\sin\sigma_5,\ 0]^T \quad (62) $$

where $\sigma_5 = \angle G_3O_2O_3$, and ${}^3\mathbf{F}_0^3$ is specified by (36).

$$ {}^3\mathbf{p}_{0L} - {}^3\mathbf{p}_{02} = [L_{O2L}\cos\sigma_6,\ L_{O2L}\sin\sigma_6,\ 0]^T \quad (63) $$

where $\sigma_6 = \angle LO_2O_3$ and

$$ {}^3\mathbf{F}_{LK} = [F_{LK}\cos\varepsilon_4,\ F_{LK}\sin\varepsilon_4,\ 0]^T \quad (64) $$

ε_4 is the angle that $\overline{LK}$ makes with a line that is parallel with the x_3-axis.

$$ {}^3\mathbf{p}_{0J} - {}^3\mathbf{p}_{02} = [L_{O2J}\cos(\sigma_7),\ L_{O2J}\sin(\sigma_7),\ 0]^T \quad (65) $$

where $\sigma_7 = \angle JO_2O_3$ is a constant angle. The components of ${}^3\vec{\mathbf{F}}_{JK}$ in the x_3- and y_3-directions emanating from point J are

$$ {}^3\mathbf{F}_{JK} = [F_{JK}\cos\gamma_1,\ F_{JK}\sin\gamma_1,\ 0]^T \quad (66) $$

where $\gamma_1 = \angle CJL + \angle LJK - (\pi - \sigma_7)$ is the angle that $\overline{JK}$ makes with a line that is parallel to the x_3-axis, and $\angle CJL$ is a constant angle; angle $\angle LJK$ is determined by the cosine theorem

$$L_{LK}^2 = L_{JK}^2 + L_{JL}^2 - 2L_{JK}L_{JL}\cos(\angle LJK) \quad (67)$$

The moment arm of ${}^3\vec{\mathbf{F}}_{FI}$ is

$${}^3\mathbf{p}_{0F} - {}^3\mathbf{p}_{02} = [L_{O_2F}\cos\sigma_8,\ L_{O_2F}\sin\sigma_8,\ 0]^T \quad (68)$$

where $\sigma_8 = \angle FO_2O_3$. The components of ${}^3\vec{\mathbf{F}}_{FI}$ in the x_3- and y_3-directions are

$${}^3\mathbf{F}_{FI} = [F_{FI}\cos\gamma_2,\ F_{FI}\sin\gamma_2,\ 0]^T \quad (69)$$

where γ_2 = angle that line segment $\overline{FI}$ makes with a line parallel to the positive x_3-axis; specifically, $\pi - \gamma_2 = \angle ICO_3 = \pi - [2\pi - \theta_3 - (\pi - \beta_3 - \angle IAC) + \angle FIC]$, angles $\beta_3 = \angle AIC$ and $\angle IAC$ are constant, and $\angle FIC$ is determined by

$$L_{FC}^2 = L_{FI}^2 + L_{CI}^2 - 2L_{FI}L_{CI}\cos(\angle FIC) \quad (70)$$

Force ${}^3\vec{\mathbf{F}}_0^3$ and moment $\vec{\mathbf{M}}_0^3$ are given in (36) and (37), respectively. Thus, all terms in (59) have been specified, and the equation of motion for link 3 is determined.

The forces at point K will next be balanced. It is assumed that the masses of the short links ($\overline{KJ}$, $\overline{KL}$, $\overline{KP}$) are negligible. The force balance equation at point K and the moment equation about point L yield, respectively,

$$-{}^3\vec{\mathbf{F}}_{LK} - {}^3\vec{\mathbf{F}}_{JK} - {}^3\vec{\mathbf{F}}_{PK} = 0 \quad (71)$$

where the forces are expressed in the third coordinate frame, for convenience. In the component form, (71) gives

$$\begin{pmatrix} F_{LK}\cos\varepsilon_4 \\ F_{LK}\sin\varepsilon_4 \end{pmatrix} + \begin{pmatrix} F_{JK}\cos\gamma_1 \\ F_{JK}\sin\gamma_1 \end{pmatrix} + \begin{pmatrix} F_{PK}\cos(\theta_{23} - \varepsilon_5) \\ F_{PK}\sin(\theta_{23} - \varepsilon_5) \end{pmatrix} = 0 \quad (72)$$

Since F_{JK} represents an input, (72) is solved for F_{PK} and F_{LK} in terms of F_{JK}

$$F_{PK} = F_{JK}\left[\frac{\sin\gamma_1 + \cos\gamma_1\tan\varepsilon_4}{\sin(\theta_{23} - \varepsilon_5) - \tan\varepsilon_4\cos(\theta_{23} - \varepsilon_5)}\right] \quad (73)$$

$$F_{LK} = F_{JK}\left[\frac{\tan(\theta_{23} - \varepsilon_5)\cos\gamma_1 + \sin\gamma_1}{\sin\varepsilon_4 - \cos\varepsilon_4\tan(\theta_{23} - \varepsilon_5)}\right] \quad (74)$$

Thus, forces F_{PK} and F_{LK} have been expressed as functions of the input F_{JK}. Therefore, expressions (73) and (74) can be substituted in equations (52) and (59).

For link 2 ($i = 2$), (9) and (10) are:

$${}^2\vec{\mathbf{F}}_{12} = {}^2\vec{\mathbf{F}}_{23} + {}^2\vec{\mathbf{F}}_{FI} - {}^2\vec{\mathbf{F}}_{BE} - {}^2\vec{\mathbf{F}}_0^2 \quad (75)$$

$$\vec{\mathbf{M}}_{12} = \vec{\mathbf{M}}_{23} - ({}^2\vec{\mathbf{p}}_{02} - {}^2\vec{\mathbf{p}}_{0G2}) \times {}^2\vec{\mathbf{F}}_{23} + ({}^2\vec{\mathbf{p}}_{01} - {}^2\vec{\mathbf{p}}_{0G2}) \times {}^2\vec{\mathbf{F}}_{12} + \vec{\mathbf{M}}_0^2 - ({}^2\vec{\mathbf{p}}_{0I} - \vec{\mathbf{p}}_{0G2}) \times {}^2\vec{\mathbf{F}}_{FI} + (\vec{\mathbf{p}}_{0B} + \vec{\mathbf{p}}_{0G2}) \times {}^2\vec{\mathbf{F}}_{BE} \quad (76)$$

Eqs. (57), (75), and (76) are next combined to obtain

$${}_s\vec{\mathbf{M}}_{12} = \vec{\mathbf{M}}_{23} - ({}^2\vec{\mathbf{p}}_{02} - {}^2\vec{\mathbf{p}}_{01}) \times {}_r^2\vec{\mathbf{F}}_{23} + ({}^2\vec{\mathbf{p}}_{0G2} - \vec{\mathbf{p}}_{01}) \times {}^2\vec{\mathbf{F}}_0^2 + \mathbf{M}_0^2 \quad (77)$$

$${}_s\vec{\mathbf{M}}_{12} = \vec{\mathbf{M}}_{12} - ({}^2\vec{\mathbf{p}}_{01} - {}^2\vec{\mathbf{p}}_{0I}) \times {}^2\vec{\mathbf{F}}_{FI} - ({}^2\vec{\mathbf{p}}_{0B} - {}^2\vec{\mathbf{p}}_{01}) \times {}^2\vec{\mathbf{F}}_{BE} - ({}^2\vec{\mathbf{p}}_{02} - {}^2\vec{\mathbf{p}}_{01}) \times {}^2\vec{\mathbf{F}}_{FI} \quad (78)$$

where ${}_r^2\vec{\mathbf{F}}_{23} = {}^2\vec{\mathbf{F}}_{23} + {}^2\vec{\mathbf{F}}_{FI} = {}^2\vec{\mathbf{F}}_{45} - {}^2\vec{\mathbf{F}}_0^3 - {}^2\vec{\mathbf{F}}_0^4$. Moment $\vec{\mathbf{M}}_{23}$ and force ${}^2\mathbf{F}_0^2$ in (77) are specified by (58) and (28), respectively. Also

$$({}^2\vec{\mathbf{p}}_{02} - {}^2\vec{\mathbf{p}}_{01}) \times {}_r^2\vec{\mathbf{F}}_{23} = L_{O_1O_2}({}_r^2F_{23y})\vec{\mathbf{k}}_z \quad (79)$$

and ${}^2F_{23y} = Y_2$-directional component of $\mathbf{F}_{23}$ in (57). $\sigma_9 = \angle G_2O_1O_2$ and $\sigma_{10} = +\angle IO_1O_2$, then

$${}^2\mathbf{p}_{0G2} - {}^2\mathbf{p}_{01} = [L_{O_1G_2}\cos\sigma_9,\ L_{O_1G_2}\sin\sigma_9,\ 0]^T \quad (80)$$

$${}^2\mathbf{p}_{01} - {}^2\mathbf{p}_{0I} = [L_{O_1I}\cos\sigma_{10},\ L_{O_1I}\sin\sigma_{10},\ 0]^T \quad (81)$$

$${}^2\mathbf{F}_{FI} = \mathbf{R}_2^3({}^3\mathbf{F}_{FI})$$

$$= [F_{FI}(\cos\gamma_2 c_3 + \sin\gamma_2 s_3),\ F_{FI}(-\cos\gamma_2 s_3 + \sin\gamma_2 c_3),\ 0]^T$$

$$= [F_{FI}\cos(\gamma_2 - \theta_3),\ F_{FI}\sin(\gamma_2 - \theta_3),\ 0]^T \quad (82)$$

By denoting $\sigma_{11} = \angle BO_1O_2$, then

$${}^2\mathbf{p}_{0B} - {}^2\mathbf{p}_{01} = [L_{O_1B}\cos\sigma_{11},\ L_{O_1B}\sin\sigma_{11},\ 0]^T \quad (83)$$

If ρ is the angle that $\overline{BE}$ makes with the positive x_2-axis, then

$${}^2\mathbf{F}_{BE} = [F_{BE}\cos(\rho - \theta_2),\ F_{BE}\sin(\rho - \theta_2),\ 0]^T \quad (84)$$

$$\rho = \tan^{-1}\{[L_{AB}\sin(\theta_2 + \sigma_{11}) + L_{AH}] / [L_{AB}\cos(\theta_2 + \sigma_{11}) + L_{EH}]\} \quad (85)$$

Moment $\mathbf{M}_0^2$ is given in (29). Thus, all terms on the right side of (77) are determined. Eq. (77) specifies the motion of link 2.

APPENDIX III. REACTION FORCE

During the digging operation, the reaction force on the edge of the bucket is determined by (Alekseeva et al. 1985)

$$F_r = k_p\left[k_s bh + \mu N + \varepsilon\left(1 + \frac{v_s}{v_b}\right)bh\sum_i \Delta x_i\right] \quad (86)$$

where k_p and k_s = specific resistances in cutting silty clay; constants b and h = width and thickness of the cut slice of soil, respectively; μ = coefficient of friction between the bucket and the soil; N = pressure force of the bucket with the soil; ε = coefficient of resistance experienced in filling the bucket during the movement of the prism of soil; V_s and V_b = volumes of the prism of soil and the bucket, respectively; and Δx = increment along the horizontal axis (in meters).

The reaction force is defined to be parallel to the digging direction. Its horizontal (F_h) and vertical (F_v) components with respect to the soil are related as: $F_h = F_r\cos(\theta_{dg} - 0.1)$; $F_v = F_r\sin(\theta_{dg} - 0.1)$ (Vähä et al. 1991). Then, the tangential component $F_t = F_r\cos(0.1)$ and the normal component $F_n = -F_r\sin(0.1)$ can be calculated.

APPENDIX IV. PARAMETERS USED IN SIMULATIONS

The numerical values of the parameters used in the simulations are as follows.

The lengths of the links are: $a_1 = 0.05$ m; $a_2 = 5.16$ m; $a_3 = 2.59$ m, $a_4 = 1.33$ m. The controller gains are: $K_p = 638{,}863$ and $K_v = 800$. The distances between points (Fig. 1) described by the subscripts are: $d_{AB} = 2.71$ m; $d_{AH} = 0.56$; $d_{AI} = 2.6$ m, $d_{AP} = 2.5$ m; $d_{CF} = 0.77$ m; $d_{CI} = 2.8$ m; $d_{CJ} = 0.63$ m; $d_{CL} = 0.63$ m; $d_{CQ} = 0.37$ m; $d_{DG} = 0.4$ m, $d_{DP} = 0.5$ m; $d_{DR} = 0.65$ m; $d_{DJ} = 2.23$ m; $d_{EH} = 0.42$ m.

The angles between the line indicated by the two subscripted letters are: DR-DN, $\sigma_4 = 0.3933$ rad; DQ-QC, $\sigma_5 = 0.3316$ rad; LC-CD, $\sigma_6 = 0.1536$ rad; JC-CD, $\sigma_7 = 1.4661$ rad; FC-CD, $\sigma_8 = 2.7105$ rad; CA-AI, $\sigma_{10} = 0.4782$ rad; BA-AC, $\sigma_{11} = 0.4957$ rad; DJ-JK, $\gamma_1 = \pi/6 - \theta_4$ rad; DF-FI, $\gamma_2 = \pi - \theta_3$ rad; $\varepsilon_2 = \theta_4$; DL-LK, $\varepsilon_4 = \pi/2 - \theta_4$ rad; DP-PK, $\varepsilon_5 = \pi/6 - \theta_4/2$ rad; BE-EH, $\rho = \pi - \tan^{-1}\{[d_{AH} + d_{AB}\sin(\theta_2 + \sigma_{11})]/[d_{AB}\cos(\theta_2 + \sigma_{11}) - d_{EH}]\}$.

The inertial moments: $I_{02} = 14{,}250.6$ kg m^2; $I_{03} = 727.7$ kg m^2; $I_{04} = 224.6$ kg m^2. The link masses: $m_2 = 1{,}566$ kg;

m_3 = 735 kg; m_4 = 432 kg. The specific resistances to cutting for silty clay: k_p = 1.0005; k_s = 5,500. The width and thickness of the cut slice of soil respectively: b = 0.61 m, h = 0.5 m. The coefficient of friction of the bucket with the soil: μ = 0.1. The pressure force of the bucket with the soil: N = 1 kg m/s^2. The coefficient of resistance to filling the bucket and movement of the prism of soil: ε = 55,000 kg/(m^2/s^2). The volume of the bucket: V_b = 0.58 m^3. The soil density: $\gamma_{\text{siltyclay}}$ = 1,921.8 kg/m^3.

APPENDIX V. REFERENCES

Alekseeva, T. V., Artem'ev, K. A., Bromberg, A. A., Voitsekhouskii, R. I., and Ul'yanov, N. A. (1985). *Machines for earthmoving work, theory and calculations*. Amerind Publishing Co. Pvt. Ltd., New Delhi, India.

Bernold, L. E. (1991). "Experimental studies on mechanics of lunar excavation." *J. Aerosp. Engrg.*, ASCE, 4(1), 9–22.

Bullock, M. D., Apte, M. S., and Oppenheim, I. J. (1990). "Force and geometry constraints in robot excavation." *Proc., Space '90, Engrg., Constr. and Operations in Space II*, ASCE, New York, N.Y., 960–969.

Hemami, A., and Daneshmend, L. (1992). "Force analysis for automation of the loading operation in a LHD-loader." *Proc., 1992 IEEE Int. Conf. on Robotics and Automation*, IEEE, Piscataway, N.J., 645–650.

Khoshzaban, M., Sassani, F., and Lawrence, P. D. (1992). "Autonomous kinematic calibration of industrial hydraulic manipulators." *Proc., 4th Int. Symp. on Robotics and Manufacturing (ISRAM'92)*, Santa Fe, N.M., ASME Press, New York, N.Y., 577–584.

Koivo, A. J. (1989). *Fundamentals for control of robotic manipulators*. J. Wiley and Sons, Inc., New York, N.Y., 42–49, 280–287.

Koivo, A. J. (1994). "Kinematics of excavators (backhoes) for transferring surface material." *J. Aerosp. Engrg.*, ASCE, 7(1), 17–32.

Seward, D. W., Bradley, D. A., and Bracewell, R. H. (1988). "The development of research models for automatic excavation." *Proc., 5th Int. Symp. on Robotics in Constr.*, Japan Ind. Robot Assoc., Tokyo, Japan, 703–708.

Sundareswaran, S., and Arditi, D. (1988). "Current state of automation and robotics in construction." *Proc., 5th Int. Symp. on Robotics in Constr.*, Japan Ind. Robot Assoc., Tokyo, Japan, 175–184.

Vähä, P. K., Koivo, A. J., and Skibniewski, M. J. (1991). "Excavation dynamics and effects of soil in digging." *Proc., 8th Int. Symp. on Automation and Robotics in Constr., ISARC-8*, Stuttgart, Germany, June 1991.

Vähä, P. K., and Skibniewski, M. J. (1993). "Dynamic model of excavator." *J. Aerosp. Engrg.*, ASCE, 6(2), 148–158.

Ward, C. J. (1988). "Equipment automation and its impact on construction technology." *Proc. ASCE Spring Conv.*, ASCE, New York, N.Y., 24–36.

Wohlford, W. P., Griswold, F. D., and Bode, B. D. (1990). "New capability for remote controlled excavation." *Proc., 38th Conf. on Remote Systems Technol.*, American Nuclear Society, La Grange Park, Ill., 228–232.

APPENDIX VI. NOTATION

The following symbols are used in this paper:

C_{ij} = (i, j) element of Coriolis and centripetal torque $\mathbf{C}(\boldsymbol{\theta}, \dot{\boldsymbol{\theta}})\dot{\boldsymbol{\theta}}$;

c_i, s_i = $\cos\theta_i$, $\sin\theta_i$, respectively;

c_{ij}, s_{ij} = $\cos(\theta_i + \theta_j)$, $\sin(\theta_i + \theta_j)$, respectively;

D_{ij} = (i, j) element of (pseudo) inertia matrix $\mathbf{D}(\boldsymbol{\theta})$;

d_i = offset distance in link i;

F_{BE} = piston force of hydraulic activator connected between B and E;

$\mathbf{F}_{\text{load}}$ = loading force acting on bucket;

F_n = normal reaction force;

F_t = tangential reaction force;

${}^i\mathbf{F}^{\text{ext}}$ = external force acting on link i;

${}^i\mathbf{F}_0^i$, ${}^i\mathbf{M}_0^i$ = force and torque, respectively, acting on gravity center of link i expressed in the ith coordinate frame;

${}^i\mathbf{F}_{(i-1)i}$, ${}^i\mathbf{M}_{(i-1)i}$ = force and torque, respectively, acting on link i from link $(i - 1)$;

G_i = ith component of gravity torque $\mathbf{G}(\boldsymbol{\theta})$;

I_i = moment of inertia of link i about centroidal axis parallel to z_i-axis;

$\vec{\mathbf{k}}_{zi}$ = unit vector on the z_i-axis;

L_{AB} = length of line segment joining points A and B, and A, B signify any two points on excavator;

l_i = a_i = length of line segment between O_{i-1} and O_i, i = 2, 3;

m_i = mass of link i;

${}^i\mathbf{p}_{0Gi}$, ${}^i\mathbf{v}_{0Gi}$, ${}^i\mathbf{a}_{0Gi}$ = position, translational velocity, and acceleration, respectively, of the gravity center of link i expressed in ith coordinate frame;

${}^{i+1}\mathbf{v}_{0i}$, ${}^{i+1}\mathbf{a}_{0i}$ = translational velocity and acceleration, respectively, of the origin of the ith coordinate frame in $(i + 1)$th coordinate system;

X_i, Y_i, Z_i = ith coordinate system, i = W, 0, 1, 2, 3, 4;

α_i = offset angle of link i;

Γ_{ij} = (i, j) element of control matrix $\boldsymbol{\Gamma}(\boldsymbol{\theta})$;

γ_1 = angle between $\overline{\text{JK}}$ and positive x_3-axis;

γ_2 = angle between $\overline{\text{IF}}$ and positive x_3-axis;

ε_4 = angle between $\overline{\text{LK}}$ and positive x_3-axis;

ε_5 = angle between $\overline{\text{PK}}$ and positive x_1-axis;

θ_b = $\theta_{234} - \pi - \theta_{dg}$ (angle between bucket bottom and X_4-axis);

θ_{dg} = angle between bucket edge and horizontal line (digging angle);

θ_i, $\dot{\theta}_i$, $\ddot{\theta}_i$ = the angular, velocity and acceleration of joint i, respectively;

θ_{ij} = $\theta_i + \theta_j$;

θ_{ijk} = $\theta_i + \theta_j + \theta_k$;

ξ = $\varepsilon_5 + \theta_{234} - \angle\underline{\text{PO}_5\text{O}_4}$;

ρ = angle between $\overline{\text{EB}}$ and positive x_3-axis;

σ_1 = $\angle\text{G}_2\text{O}_2\text{O}_1$;

σ_2 = $\angle\text{G}_3\text{O}_3\text{O}_2$;

σ_2 = $\angle\text{G}_4\text{O}_4\text{O}_3$;

σ_4 = $\angle\text{G}_4\text{O}_3\text{O}_4$;

σ_5 = $\angle\text{G}_3\text{O}_2\text{O}_3$;

σ_6 = $\angle\text{LO}_2\text{O}_3$;

σ_7 = $\angle\text{JO}_2\text{O}_3$;

σ_8 = $\angle\text{FO}_2\text{O}_3$;

σ_9 = $\angle\text{G}_2\text{O}_1\text{O}_2$;

σ_{10} = $\angle\text{IO}_1\text{O}_2$;

σ_{11} = $\angle\text{BO}_1\text{O}_2$; and

${}^{i+1}\boldsymbol{\omega}_i$, ${}^{i+1}\boldsymbol{\alpha}_{0i}$ = angular velocity and acceleration, respectively, of ith coordinate frame in the $(i + 1)$th coordinate system.